AN EMPIRICAL MODEL FOR A PIEZOELECTRIC TISSUE CONTRAST SENSOR EMBEDDED IN A BIOPSY TOOL

Tao Li* and Yogesh B. Gianchandani

Engineering Research Center for Wireless Integrated Microsystems
University of Michigan, Ann Arbor, USA

ABSTRACT

This paper describes an empirical model for a micromachined piezoelectric sensor located in a hollow cavity on the interior tip of a biopsy needle to aid in real time tissue differentiation during fine needle aspiration (FNA) biopsy. The disc-shaped sensor made from bulk lead zirconate titanate (PZT) has 50 μm thickness and 200 μm diameter. Samples such as oils and saline solution with controlled acoustic impedance ranging over 1.1-1.6×10^6 Kg/m^2s were tested for calibration. A modified Butterworth-Van Dyke (BVD) equivalent circuit is used to model the PZT disc with tissue loading, and an empirical tissue contrast model shows an approximately proportional relationship between frequency shift and sample acoustic impedance.

Keywords: Piezoelectric Sensor, Resonance, BVD Circuits, Fine Needle Aspiration (FNA)

I. INTRODUCTION

While thyroid cancer results in <1% of cancer deaths, thyroid nodules, either benign or malignant, can be observed in ≈20% of the general US population [1]. Since conventional ultrasound imaging cannot generally distinguish benign and malignant nodules, FNA biopsy is usually required to make a final diagnosis. This is typically performed with a thin needle of 20-27 gauge with outer diameter <1 mm, and is challenging in itself due to the precision required in acquiring the desired sample from the small target volumes for subsequent cytological examination. To aid the positioning of the biopsy needle, traditional ultrasound imaging is performed in real time. Despite the added complexity, this does not provide the necessary precision, and at least 2-5% of FNAs are read as non-diagnostic because of improper sampling [1-3].

We recently reported an in-situ device for detecting tissue contrast during FNA biopsy of thyroid nodules [4]. Intended to complement traditional ultrasound imaging, it uses a micromachined piezoelectric sensor embedded near the tip of a biopsy needle to distinguish tissue planes in real time. However, its practical use demands a predictive model for the interaction between the device and sample. In this paper an empirical model is developed based on new experimental results obtained from samples with known acoustic impedance.

II. DEVICE DESCRIPTION

The scheme for in-situ detection of tissue contrast during thyroid biopsy is shown in Fig. 1. A sensor made from bulk lead zirconate titanate (PZT) is integrated at the tip of the needle and is connected to a spectrum analyzer for real-time impedance measurement. Figure 2 illustrates the structure of the device. The creation of the cavity in the wall of the biopsy needle (Fig. 2b) leaves a thin, tailored, stainless steel diaphragm. A micromachined PZT disc (Fig. 2c) is located against the diaphragm (Fig. 2d). The varying acoustic impedance of the nearby tissue changes the vibrational characteristics of the diaphragm, and hence the mechanical boundary condition of the PZT disc. This is transduced into a change of its electrical impedance by the piezoelectric effect, and subsequently detected by the impedance spectrum analyzer, thus providing a measure of tissue contrast.

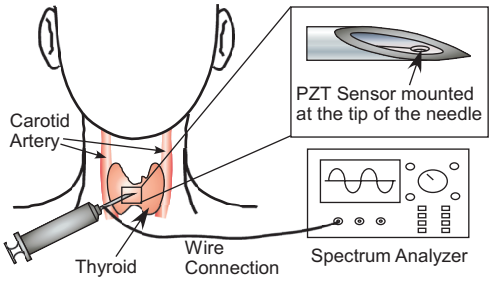

Fig. 1: Schematic of the proposed tissue contrast sensor used for thyroid biopsy.

III. MEASUREMENT RESULTS

For the purpose of device calibration and modeling, the sensor was tested with samples that have known and controlled acoustic impedance (Z_a). These are oil samples and saline solution of varying concentration.

* *Corresponding author:* 1301 Beal Ave., Ann Arbor, MI, 48109, USA; Tel: 1-734-647-2040; Email: litz@umich.edu

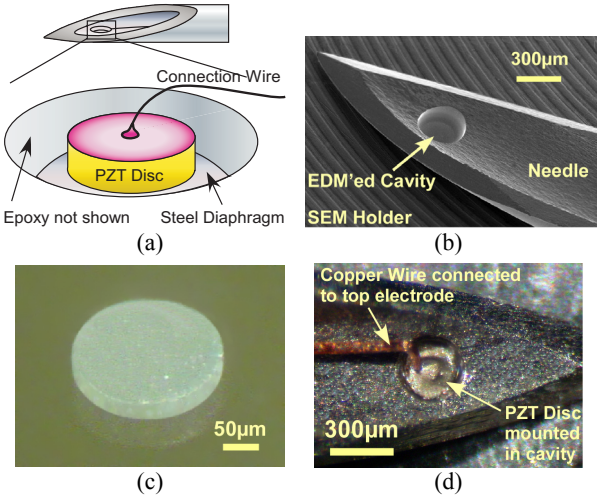

Fig. 2: (a) Schematics of the tissue contrast sensor in perspective view with sealing epoxy removed; (b) SEM image of a syringe needle tip processed by micro electro-discharge machining (µEDM) to form the cavity for mounting PZT sensor. (c) Photo of a released PZT disc batch fabricated by SEDUS process [5] using batch micro ultrasonic machining to transfer a pattern defined by serial µEDM. Diameter: 200 µm. Thickness: 50 µm. (d) Finished device before sealing epoxy is applied. Coated copper wire is used to make connection to the top electrode of the PZT disc. The stainless steel needle body is used as the ground electrode.

The sensor response was measured at a needle insertion depth of 5 mm for all cases. The Z_a of these samples ranged over 1.1-1.6×10^6 Kg/m^{2}s, with Z_a of common tissues toward the upper end of this range. In the experiment with saline samples, solution concentrations from 1% to 20% were tested; the measurement results are shown in Fig. 3. The measured frequency shift increased with greater saline concentration when the concentration was smaller than ≈3.5%, and remained approximately constant when the concentration became greater. This phenomenon is similar to that discussed in [6], and is possibly due to saturation of available cation binding cites on the sensor diaphragm. The sample acoustic properties obtained from literature and the experimental results of resonance frequency shift are used for the subsequent device modeling.

IV. DEVICE MODELING

The resonance frequency shift (Δf) of the piezoelectric sensor is dependent on both the mass loading effect and elastic properties of the samples [7]. The Z_a of a sample is the product of its density and acoustic velocity, the latter being further related to the elastic bulk modulus of the material. Thus, an empirical tissue contrast model can be built for the biopsy device by plotting the measured Δf versus Z_a, as shown in Fig. 4(a). The data used in this plot are from results described in Section III and previous results for porcine fat and muscle tissue discussed in [4]. The relationship is approximately proportional, as shown in the shaded area, considering the uncertainty in the acoustic properties of the samples.

The electrical characteristics of a free PZT disc in longitudinal vibration mode can be modeled by a lumped-element Butterworth-Van Dyke (BVD) equivalent circuit as shown in Fig. 5(a) [8]. In this circuit, C_0 is the clamped capacitance between the two electrodes of the PZT disc, and an infinite number of series LC_n (n=1,3,5…) motional branches are connected in parallel, where n denotes harmonic modes of the mechanical

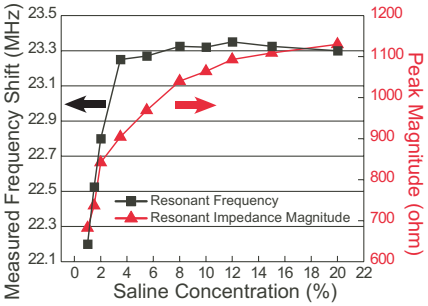

Fig. 3: Measurement results of saline sample with concentration between 1% and 20% shown as measured frequency shift and peak magnitude of impedance vs. saline concentration.

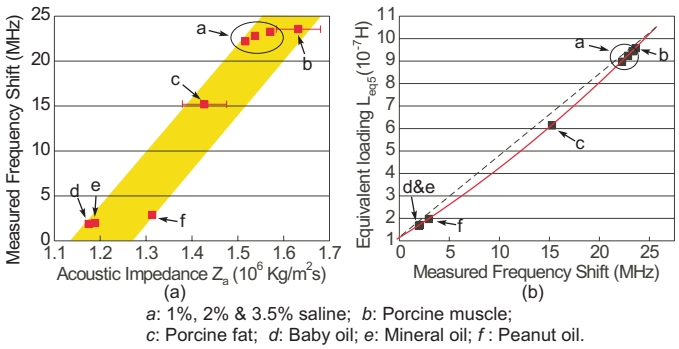

Fig. 4: (a) Measured resonant frequency shift vs. acoustic impedance of the samples. The error bars on the data for porcine samples indicate lack of certainty in the values of acoustic impedance Z_a. (b) Calculated equivalent loading L_{eq5} as a function of frequency shift for the samples. The dotted line indicates linear relation for comparison.

resonance of the disc. The first branch of L and C_1 corresponds to the fundamental resonance mode, and the n^{th} branch of L and C_n represents the n^{th} mode. The equations to determine the values of C_0, L, and C_n can be found in [8].

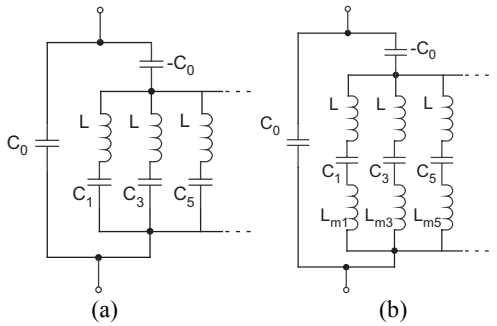

Fig. 5: BVD equivalent circuits of a piezoelectric resonator in longitudinal vibration mode. All loss mechanism ignored. (a) free resonance; (b) with equivalent loading.

A modification to this original BVD circuit is necessary to accommodate the loading effect. Inductors can be used to model mass loading such as a diaphragm attached to a piezoelectric sensor [7]. These inductors are denoted as $L_{m(n)}$ in Fig. 5(b), and their values for such a diaphragm loading can be determined using equations provided in [7]. To include the tissue loading effect in the model, $L_{m(n)}$ can be extended by adding in series another equivalent loading inductance $L_{eq(n)}$. This additional inductance is an equivalent that includes the effect of both mass and elastic loading for modeling convenience. The frequency of each harmonic mode $f_{(n)}$, or equivalently the frequency of each electrical impedance peak can then be denoted as

$$f_{(n)} = \frac{1}{2\pi\sqrt{(L + L_{m(n)} + L_{eq(n)})C_n}}, n = 1,3,5... \quad (1)$$

In the experiments, the 5th harmonic mode (at 176 MHz in air) was found to have a higher Q than the fundamental and 3rd harmonic mode, and was consequently selected for measurement. Therefore, the 3rd LC_n branch (for the 5th harmonic mode) of the modified BVD circuit is of the most interest. The calculated equivalent loading L_{eq5} for each of the samples used to build the empirical tissue contrast model is plotted as a function of the measured frequency shift Δf_5 in Fig. 4(b). The two plots in Fig. 4 provide the empirical tissue contrast model (i.e., the relationship of Z_a to Δf_5) and the relationship of L_{eq5} to Δf_5. These relationships can be used with the modified BVD circuit model to relate the physical parameters of the device and samples to Δf for design and optimization of the sensor.

V. CONCLUSIONS

An empirical model has been built for the piezoelectric tissue contrast sensor based on experimental results and a modified BVD circuit model. This model established the relationship between the measured frequency shift and sample acoustic impedance, providing an effective approach to predict the interaction between the device and sample for its proposed practical use.

ACKNOWLEDGEMENT

This work was supported primarily by the Engineering Research Centers Program of the National Science Foundation under Award Number EEC-9986866.

REFERENCES

[1] F. Pacini and L.J. De Groot, "Thyroid Neoplasia," *The Thyroid and its Diseases*, 6th ed., W.B. Saunders Company, 1996, updated online at http://www.thyroidmanager.org, May 2004

[2] S. Takashima, H. Fukuda, and T. Kobayashi, "Thyroid nodules: clinical effect of ultrasound-guided fine-needle aspiration biopsy," *J. Clin. Ultrasound,* 22(9), pp. 535-42, Nov.-Dec. 1994

[3] H. Gharib and J. R. Goellner, "Fine-needle aspiration biopsy of the thyroid: an appraisal," *Ann. Intern. Med.* 118(4), pp.282-9, Feb. 1993

[4] T. Li, R.Y. Gianchandani, and Y.B. Gianchandani, "A bulk PZT microsensor for in-situ tissue contrast detection during fine needle aspiration biopsy of thyroid nodules," *Proc. IEEE MEMS 2006*, Istanbul, pp. 12-15, Jan. 2006

[5] T. Li and Y.B. Gianchandani, "A micromachining process for die-scale pattern transfer in ceramics and its application to bulk piezoelectric actuators," *IEEE/ASME J. Microelectromechanical Systems*, 15(3), pp. 605-12, Jun. 2006

[6] H. Zhang, M.S. Marma, E.S. Kim, C.E. McKenna, and M.E. Thompson, "Implantable resonant mass sensor for liquid biochemical sensing," *Proc. IEEE MEMS 2004*, pp. 347-50, Jan. 2004

[7] H. Zhang, E.S. Kim, "Micromachined acoustic resonant mass sensor," *IEEE/ASME J. Microelectromechanical Systems*, 14(4), pp. 699-706, Aug. 2005

[8] T. Ikeda, *Fundamentals of Piezoelectricity*, Oxford University Press, New York, 1990